

ENHANCED TIDAL DISRUPTION RATES FROM MASSIVE BLACK HOLE BINARIES

XIAN CHEN^{1,2}, PIERO MADAU², ALBERTO SESANA³, & F. K. LIU^{1,4}

ABSTRACT

“Hard” massive black hole (MBH) binaries embedded in steep stellar cusps can shrink via three-body slingshot interactions. We show that this process will inevitably be accompanied by a burst of stellar tidal disruptions, at a rate that can be several orders of magnitude larger than that appropriate for a single MBH. Our numerical scattering experiments reveal that: 1) a significant fraction of stars initially bound to the primary hole are scattered into its tidal disruption loss cone by gravitational interactions with the secondary hole, an enhancement effect that is more pronounced for very unequal-mass binaries; 2) about 25% (40%) of all strongly interacting stars are tidally disrupted by a MBH binary of mass ratio $q = 1/81$ ($q = 1/243$) and eccentricity 0.1; and 3) two mechanisms dominate the fueling of the tidal disruption loss cone, a Kozai non-resonant interaction that causes the secular evolution of the stellar angular momentum in the field of the binary, and the effect of close encounters with the secondary hole that change the stellar orbital parameters in a chaotic way. For a hard MBH binary of $10^7 M_\odot$ and mass ratio 10^{-2} , embedded in an isothermal stellar cusp of velocity dispersion $\sigma_* = 100 \text{ km s}^{-1}$, the tidal disruption rate can be as large as $\dot{N}_* \sim 1 \text{ yr}^{-1}$. This is 4 orders of magnitude higher than estimated for a single MBH fed by two-body relaxation. When applied to the case of a putative intermediate-mass black hole inspiraling onto Sgr A*, our results predict tidal disruption rates $\dot{N}_* \sim 0.05 - 0.1 \text{ yr}^{-1}$.

Subject headings: black hole physics – methods: numerical – stellar dynamics

1. INTRODUCTION

Close massive black hole (MBH) binaries are expected to form in large numbers following the hierarchical assembly of massive galaxies (e.g. Begelman et al. 1980; Volonteri et al. 2003), but their merger history remains poorly understood. Few observational probes of the processes that lead to and accompany the shrinking and inspiral of a MBH binary have been proposed to date: 1) the gravitational slingshot ejection of hypervelocity stars from the Galactic Center into the halo (e.g. Yu & Tremaine 2003; Levin 2006; Sesana et al. 2006, 2007; Brown et al. 2009; Perets 2009); 2) interruption or redirection of jets due to MBH binary-accretion disk interaction or MBH coalescence (Merritt & Ekers 2002; Liu et al. 2003; Liu 2004; Liu & Chen 2007); 3) the coalescence of MBH pairs with masses in the range $(10^4 - 10^7)/(1+z) M_\odot$ giving origin to gravitational wave events that are one of the primary targets for the planned *Laser Interferometer Space Antenna (LISA)*; e.g. Haehnelt 1994; Hughes 2002; Wyithe & Loeb 2003; Sesana et al. 2004, 2005); 4) the electromagnetic afterglow from a circumbinary accretion disk that would follow such coalescence (e.g. Milosavljević & Phinney 2005; Dotti et al. 2006; Lippai et al. 2008; Shields & Bonning 2008); and 5) the high-velocity recoil experienced by the plunging binary due to the asymmetric emission of gravitational waves (e.g. Baker et al. 2008, and references therein). A recoiling hole that retains the inner

parts of its accretion disk may have fuel for a long-lasting luminous phase along its trajectory, and shine as an off-center AGN (e.g. Madau & Quataert 2004; Blecha & Loeb 2008; Volonteri & Madau 2008).

In this *Letter* we return to the dynamical processes that determine the decay of MBH binaries in a stellar background, prior to the gravitational wave regime, and put forward another possible observational signature of close binaries in the nuclei of galaxies. Using results from scattering experiments we show that gravitational slingshot interactions between an unequal-mass “hard” binary and a bound stellar cusp will inevitably be accompanied by a burst of stellar tidal disruptions, at a rate that can be *several orders of magnitude larger* than that appropriate to a single MBH fed by two-body relaxation. The duration of the phase of enhanced tidal disruption is of the order of $10^4 - 10^5 \text{ yr}$.

2. SCATTERING EXPERIMENTS

Analytical techniques have been used by Ivanov et al. (2005) to study the enhanced stellar disruption rates induced by the secular non-resonant interaction with a non-evolving MBH binary. Here, we perform detailed numerical experiments of the close encounters between stars and the pair of MBHs, collisions that perturb stellar orbits in a chaotic way and scatter stars initially bound to the primary MBH into its tidal disruption loss cone. Consider a MBH binary of mass $M = M_1 + M_2 = M_1(1+q)$ ($M_2 \ll M_1$) and semi-major axis a , orbiting in a background of stars of mass m_* , radius R_* , and velocity dispersion σ_* . When $a \lesssim a_h \equiv GM_2/4\sigma_*^2$, the “hard” binary loses orbital energy by three-body slingshot interactions (Quinlan 1996; Sesana et al. 2006, 2007). For unequal-mass pairs, the radius of influence $r_{\text{inf}} \equiv G(M_1 + M_2)/(2\sigma_*^2)$ is much larger than the hardening radius a_h , and almost all interacting (low angular-

¹ Department of Astronomy, Peking University, 100871 Beijing, China.

² Department of Astronomy & Astrophysics, University of California, Santa Cruz, CA 95064.

³ Center for Gravitational Wave Physics, The Pennsylvania State University, University Park, State College, PA 16802.

⁴ Kavli Institute for Astronomy and Astrophysics, Peking University, 100871 Beijing, China

momentum) stars are bound to M_1 .⁵ In the case of an isothermal stellar distribution around M_1 , the total stellar mass within a_h is equal to $M_2/2$.

The integration of the three-body encounter equations is performed in a coordinate system centered at the location of M_1 . Initially the binary (of mass ratio q) has eccentricity e and a randomly-oriented orbit with M_2 at its pericenter. Stars initially move in the $x-y$ plane with pericenters along the positive x -axis and random orbital phases. The initial conditions of the restricted three-body problem are then completely defined by 6 variables, 3 for the binary and 3 for the star: 1) the inclination of the binary orbit, θ ; 2) the longitude of M_2 's ascending node, l ; 3) the argument of M_2 's pericenter, ϕ ; 4) the semi-major axis of the stellar orbit, a_* ; 5) the specific angular momentum of the star, j_* ; and 6) the orbital phase of the star, p_* . We start each scattering experiment by generating 6 random numbers, with $\cos\theta$ evenly sampled in the range $[-1, 1]$, and l and ϕ uniformly distributed in the range $[0, 2\pi]$. We sample a_* logarithmically around a in the range $[1/2a, 2a]$ where three-body interactions are strongest, j_*^2 randomly between 0 and 1 (corresponding to an isotropic distribution), and p_* evenly between 0 and 1. The equation of motion are integrated using an explicit Runge-Kutta method of order 8 (Hairer et al. 1987), with a fractional error per step in position and velocity set to 10^{-13} . We have tested our code by reproducing Figures 4 and 6 in Sesana et al. (2008) and found excellent agreement, and run 10^4 scattering experiments for each binary configuration. During each experiment the minimum separation r_{\min} between the star and the MBH pair is measured and stored: stars on orbits intersecting the tidal radius of hole M_i ($i = 1, 2$),

$$r_{ti} = r_* \left(\frac{M_i}{m_*} \right)^{1/3} \simeq (2.3 \times 10^{-6} \text{ pc}) \left(\frac{r_*}{R_\odot} \right) \left(\frac{M_i}{10^6 m_*} \right)^{1/3}, \quad (1)$$

will be tidally disrupted at pericenter passage (neglecting general relativistic effects that set in when $M_1 \gg 10^7 M_\odot$, see Hills 1975). The results of our numerical experiments are shown in Figure 1 for binaries with different mass ratios and eccentricities, all at separation $a = a_h$. The fraction of interacting stars that are scattered by M_2 to within a pericenter distance $r_{\min} < r_{t1}$ from M_1 and are tidal disrupted can be, for very unequal mass binaries, orders of magnitude higher than the corresponding number were M_1 not in a binary. The latter is simply given by all the bound stars within M_1 “tidal loss cone”, the region in the $(a_* - j_*)$ phase-space bounded by

$$j_{lc}^2 = \begin{cases} 1 & (a_* < r_{t1}) \\ 2(r_{t1}/a_*)^2 (a_*/r_{t1} - 1/2) & (a_* \geq r_{t1}), \end{cases} \quad (2)$$

where j_* is the specific angular momentum of the star normalized to the angular momentum of a circular orbit with the same semi-major axis. For a binary with $q = 1/81$, $e = 0.1$, the probability that a close encounter with a star having $1/2a < a_* < 2a$ results in a tidal dis-

ruption by M_1 ($r_{\min} < 3 \times 10^{-4} a \approx r_{t1}$) is more than 2 orders of magnitude larger than if M_1 were single. The figure also shows that: 1) many more stars are disrupted by M_1 than by M_2 ; 2) the disruption probability decreases with increasing q . This is both because the ratio r_{t1}/a_h decreases with increasing q , and because, as the perturbing force of the secondary increases, more stars are ejected altogether rather than disrupted; and 3) more stars are scattered into M_1 's tidal loss cone with decreasing binary eccentricity.

3. BASIC THEORY AND DISRUPTION RATES

Figure 2 shows an example of a three-body scattering leading to a tidal disruption after many pericenter passages. In the presence of a secondary black hole, strongly interacting ($a_* \sim a$) stars in nearly circular, highly inclined orbits relative to the binary orbital plane undergo a slow secular evolution that periodically increases their eccentricity (in exchange for a lower inclination) and eventually drives them within the tidal disruption loss cone of the primary hole (Ivanov et al. 2005). Our scattering experiments show that this mechanism – analogous to the so-called “Kozai effect” of celestial mechanics (Kozai 1962) – contributes but does not dominate the fueling of the tidal disruption loss cone in the case of very unequal mass binaries. The stars supplied to the disruption loss cone by the Kozai effect are all those having normal component of the angular momentum, j_{z*} , within the loss cone, i.e. all those stars within a wedge-like region in phase space where $|j_{z*}| < j_{lc}$. For a given stellar semi-major axis, $a_* \ll a$, the fraction of stars that lie outside the tidal disruption loss cone but inside the “Kozai wedge” is

$$f_K(r_{t1}, a_*) = \int_{j_{lc}}^1 dj_* \int_{-j_{lc}}^{j_{lc}} dj_{z*} = 2j_{lc} - 2j_{lc}^2. \quad (3)$$

When $r_{t1} \ll a_*$, $f_K \simeq 2\sqrt{2r_{t1}/a_*}$, which is $\sqrt{2a_*/r_{t1}}$ times larger than the fraction of stars already in the tidal loss cone, $j_{lc}^2 \simeq 2r_{t1}/a_*$. This result explains why the probability of stellar disruption for bound stars is much higher in MBH binaries than in single black hole systems. It also predicts that only a fraction $2\sqrt{2r_{t1}/a_*} = (0.05, 0.09, 0.15)$ for $q = (1/81, 2/243, 1/721)$ of all stars with $a/2 < a_* < 2a$ will be supplied to the tidal loss cone by the Kozai effect. Figure 1 shows that for very unequal mass binaries the tidal disruption probability is much larger than the above estimate. This discrepancy highlights the importance of close, resonant encounters with the secondary hole, which change the stellar orbital parameters in a chaotic way and fuel the tidal loss cone. Figure 2 (bottom right panel) depicts the initial distribution in the $(a_* - j_{z*})$ plane of all the stars that are disrupted in our numerical experiments. It is clear that the majority of disrupted stars lie outside the Kozai wedge.

We now show that the ejection of ambient stars by a hard MBH binary will be accompanied by a burst of stellar tidal disruptions, at a rate that may be orders of magnitude larger than that appropriate for a single MBH. In our numerical experiments the time when a star first crosses the tidal radius of the primary hole is stored and used to calculate a disruption frequency. To translate this number into a stellar disruption rate in

⁵ Note that, for extreme mass ratios $q \ll 1$, the encounter is essentially a two-body scattering as the star and the secondary hole move in the static potential of the primary.

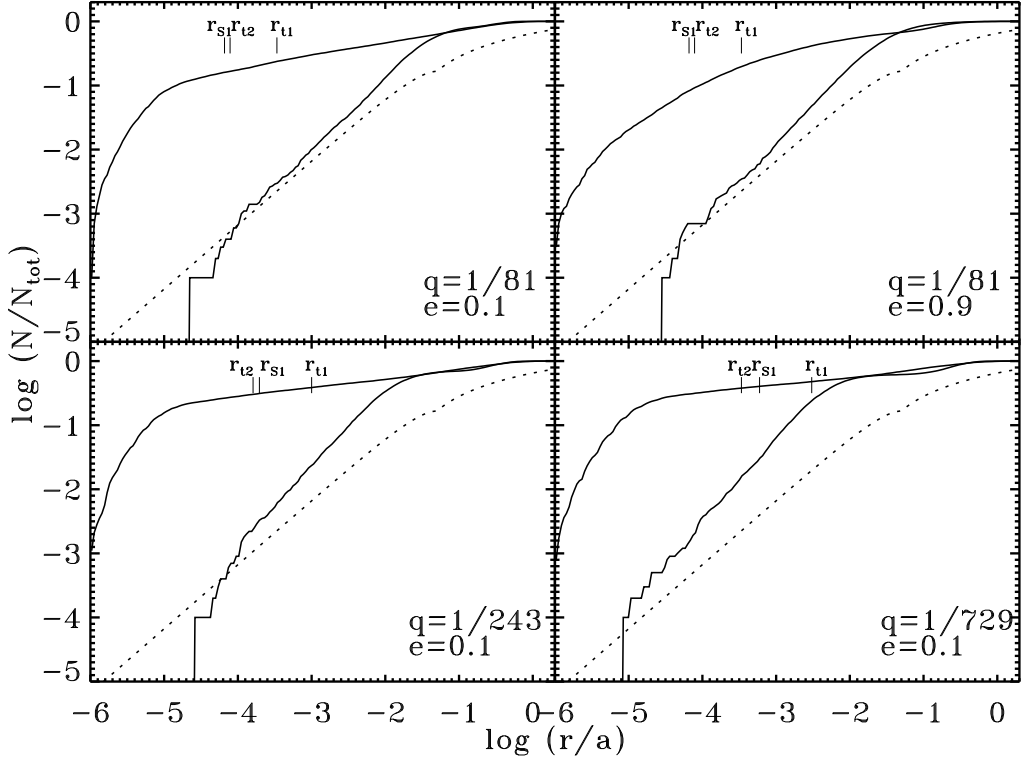


FIG. 1.— *Upper solid line*: Close-encounter probability for bound stars interacting with the primary member (of mass M_1) of a MBH binary of mass ratio q , eccentricity e , and separation $a = a_h$. The vertical axis shows the fraction of stars N/N_{tot} with closest approach distance $r_{\text{min}} < r$. *Lower solid line*: same for M_2 . *Dotted line*: same in the case of an isolated MBH of mass M_1 . Stars are drawn from a spherical isotropic distribution bound to M_1 and have semi-major axis in the range $a/2 < a_* < 2a$. The short vertical lines mark the tidal radii of M_1 and M_2 and the Schwarzschild radius of M_1 (all in units of a) for $M_1/m_* = 10^7$, $r_* = R_\odot$, and $\sigma_* = 100 \text{ km s}^{-1}$. From the top left to the bottom right, the fraction of stars tidally disrupted ($r_{\text{min}} < r_{t1}$) by M_1 is 0.24, 0.19, 0.39, and 0.48, respectively.

physical units one needs to specify the parameters of the MBH binary and its stellar cusp. At the hardening radius

$$a_h \equiv \frac{GM_2}{4\sigma_*^2} \simeq (1.1 \text{ pc}) \sigma_{100}^{-2} q M_7 \quad (4)$$

the orbital period of the binary is

$$P_h = 2\pi \sqrt{\frac{a_h^3}{G(M_1 + M_2)}} \simeq (3.3 \times 10^4 \text{ yr}) \sigma_{100}^{-3} M_7 \left(\frac{q^3}{1+q} \right)^{1/2}, \quad (5)$$

where $\sigma_{100} \equiv \sigma_*/100 \text{ km s}^{-1}$ and $M_7 \equiv M_1/10^7 M_\odot$. If we assume now, for simplicity, that the stars bound to M_1 follow an isothermal distribution, $\rho_*(r) = \sigma_*^2/(2\pi Gr^2)$, the total stellar mass between $a_h/2$ and $2a_h$ is $M_* = 3qM_1/4$. Normalizing the interacting mass in our numerical experiment to the isothermal case and rescaling the stored disruption times according to equation (5), we obtain the stellar disruption rates shown in Figure 3.

Although the standard Kozai theory does not strictly apply to strongly interacting stars, we use it here to derive an analytical scaling for the stellar disruption rates. The Kozai timescale at a_h is approximately

$$T_K = \frac{2}{3\pi q} \left(\frac{a_*}{a_h} \right)^{-3/2} P_h \quad (6)$$

(Innanen et al. 1997; Kiseleva et al. 1998). The stellar

disruption rate can then be estimated as

$$\dot{N}_* = \frac{\lambda f_K M_*}{m_* T_K} e^{-t/T_K} \quad (7)$$

$$\simeq (6 \text{ yr}^{-1}) \lambda (1+q)^{1/2} \sigma_{100}^4 M_7^{-1/3} e^{-t/T_K}, \quad (8)$$

where f_K is the fraction of stars in the Kozai wedge and $\lambda \simeq 0.2$ is a correction factor accounting for the uncertainty in T_K and for stars that are actually ejected before disruption, as well as for properly weighting our scattering experiments for the case of an isothermal profile. The numbers provided by equation (8) are in good agreement with the numerical rates. The tidal disruption plateau, however, lasts much longer than T_K (indicated by the vertical ticks in Fig. 3), because at late times the disruption rate is dominated by chaotic scatterings.

The tidal disruption rates we compute are many orders of magnitude higher than those,

$$\dot{N}_* \simeq (2 \times 10^{-4} \text{ yr}^{-1}) \sigma_{100}^{7/2} M_7^{-1} \left(\frac{m_*}{M_\odot} \right)^{-1/3} \left(\frac{r_*}{R_\odot} \right)^{1/4}, \quad (9)$$

derived for a single MBH fed by two-body relaxation (Wang & Merritt 2004). Note that in our calculations we have only considered stars with $a/2 < a_* < 2a$. Taking into account stars in a larger range of semi-major axis would further boost the binary disruption rates.

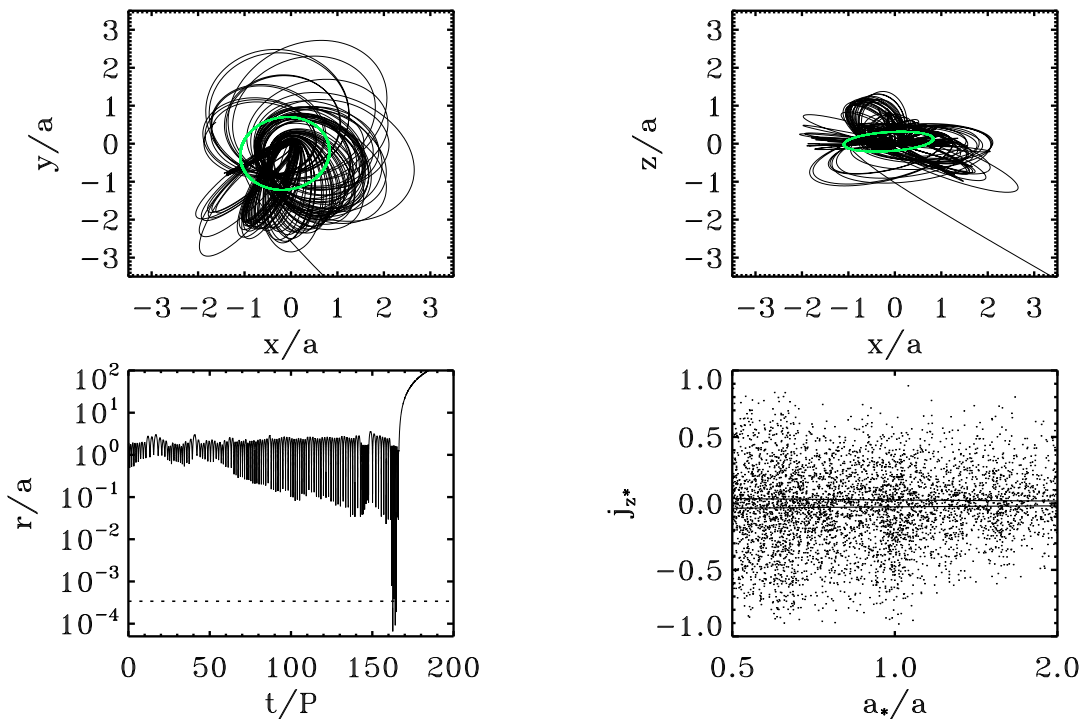


FIG. 2.— *Top and bottom left panels:* Example of a chaotic three-body scattering leading to a tidal disruption. A star on a bound orbit of semi-major axis $a_* = 1.2a$ and eccentricity $e_* = 0.5$ interacts with a MBH binary of parameters $M_1 = 10^7 M_\odot$, $q = 1/81$, $e = 0.3$, $a = a_h$. *Top left:* stellar (black) and M_2 (green) trajectories in the $x - y$ plane. The primary hole M_1 is located at the origin. *Top right:* same projected onto the $x - z$ plane. *Bottom left:* separation between the star and M_1 as a function of time (in units of the binary period P). The dotted line marks the tidal radius r_{t1} . *Bottom right panel:* Bound stars in the $(a_* - j_{z*})$ plane that are tidally disrupted during the interaction with a MBH binary of parameters $M_1 = 10^7 M_\odot$, $q = 1/81$, $e = 0.1$, $a = a_h$. The solid lines mark the boundaries of the Kozai wedge $|j_{z*}| < j_{lc}$.

4. CONCLUSIONS

We have used results from numerical scattering experiments and shown that the tidal disruption rate in a stellar cusp containing a $10^7 M_\odot$ MBH binary can be as large as 1 yr^{-1} over a timescale of $\sim 10^5 \text{ yr}$. *This is orders of magnitude larger than expected in the case of single MBHs.* After a tidal disruption, about half of the debris will be spewed into eccentric bound orbits and fall back onto the hole, giving rise to a bright UV/X-ray outburst that may last for a few years (e.g. Rees 1988). “Tidal flares” from MBHs may have been observed in several nearby inactive galaxies (Komossa 2002; Esquej et al. 2007). The inferred stellar disruption frequency is $\sim 10^{-5} \text{ yr}^{-1}$ per galaxy (with an order of magnitude uncertainty, Donley et al. 2002). The much enhanced disruption rates we have found here for MBH binaries can then be used to constrain the abundance of close MBH pairs in nearby galaxy nuclei (Chen et al. 2008). It is interesting to scale our results to the scattering of stars bound to Sgr A*, the massive black hole in the Galactic Center, by a hypothetical inspiraling companion of intermediate mass (Yu & Tremaine 2003; Sesana et al. 2007). The stellar density profile around the Galactic Center can be described as a double power-law, with outer slope $\simeq -2$ and inner slope $\simeq -1.5$ (Schodel et al. 2007). If the density profile inside the influence radius of

M_1 is shallower than isothermal,

$$\rho_*(r < r_{\text{inf}}) = \rho_*(r_{\text{inf}}) \left(\frac{r}{r_{\text{inf}}} \right)^{-\gamma} \quad (10)$$

with $\gamma < 2$, then the stellar mass between $2a_h$ and $a_h/2$ decreases by a factor $(a_h/r_{\text{inf}})^{2-\gamma}$, and the stellar disruption rate in equation (8) decreases by a factor $(q/4)^{2-\gamma}$ relative to the isothermal case. Using $M_1 = 4 \times 10^6 M_\odot$, $\sigma_* = 100 \text{ km s}^{-1}$, $\gamma = 1.5$, and $1/243 < q < 1/81$, yields rates in the range $\dot{N}_* \simeq 0.05 - 0.1 \text{ yr}^{-1}$.

There are a number of uncertainties in our calculations that require clarification before a firm statement can be made on the rates and duration of stellar tidal disruptions expected in galaxy nuclei hosting MBH binaries, and on the constraints imposed by the very low level of activity observed in the Galactic Center. First and foremost, our estimates of the tidal disruption rate assume a fixed binary separation a . In reality, both binary separations and eccentricities will evolve due to three-body slingshots (Sesana et al. 2008). This changes the Kozai timescale of the system and replenishes the supply of strongly interacting stars. According to Figure 7 of Sesana et al. (2008), the evolutionary timescale of a binary with initial eccentricity 0.1 embedded in an isother-

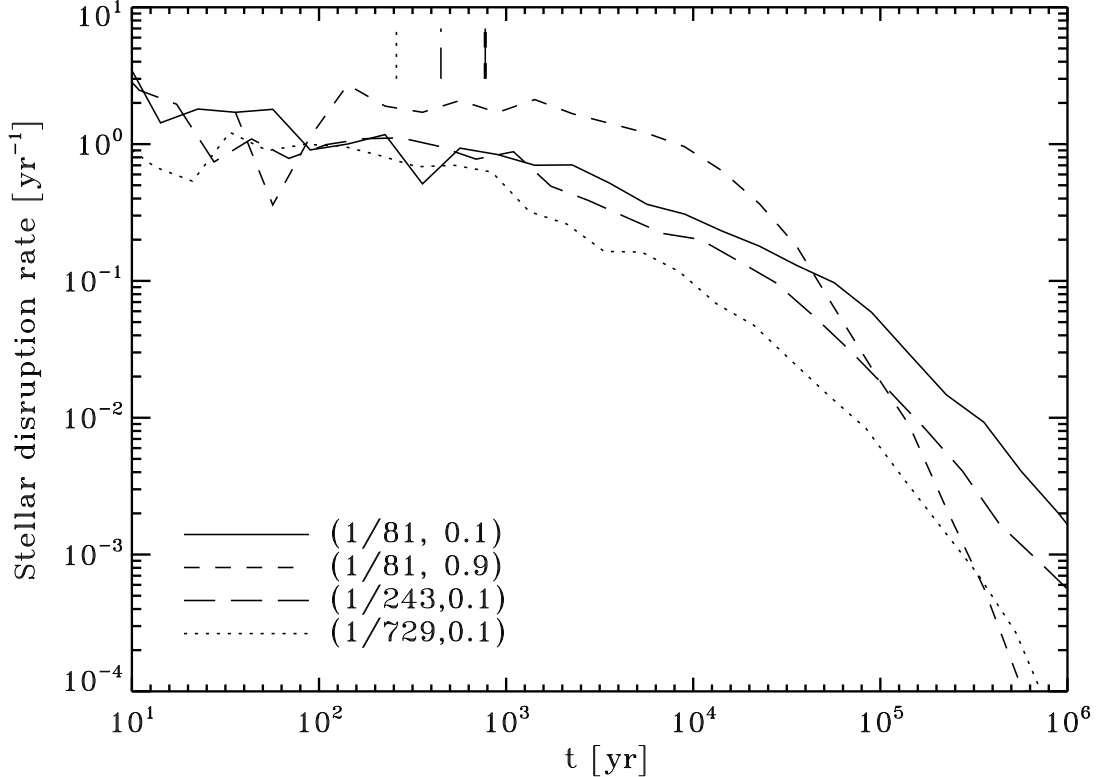


FIG. 3.— Numerical tidal disruption rates as a function of time for a hard MBH binary of mass ratio q , eccentricity e , and separation $a = a_h$, embedded in an isothermal stellar cusp. The derivation assumes $M_1 = 10^7 M_\odot$, $m_* = 1 M_\odot$, $r_* = R_\odot$, and $\sigma_* = 100 \text{ km s}^{-1}$. The short vertical lines mark the Kozai timescale for $a_* = a = a_h$.

mal cusp is $t_h \sim q^{-3/2} P$. At $a = a_h$ we derive

$$t_h \sim (3.3 \times 10^4 \text{ yr}) \sigma_{100}^{-3} M_7 (1+q)^{-1/2}. \quad (11)$$

This is comparable to the duration of the plateau in the disruption rates shown in Figure 3, implying that binary evolution should not qualitatively change the plateau values. A more sophisticated calculation that couples the results of numerical scattering experiments with an evolu-

ing binary will be the subject of a subsequent paper.

Support for this work was provided by NASA through grant NNX08AV68G (P.M.). X.C. and F.K.L. thank the Chinese national 973 program (2007CB815405) and the China Scholarship Council for financial support. We are grateful to F. Haardt for early discussions on this topic.

REFERENCES

- Baker, J. G., Boggs, W. D., Centrella, J., Kelly, B. J., McWilliams, S. T., Miller, M. C., van Meter, J. R. 2008, *ApJ*, 682, L29
- Begelman, M. C., Blandford, R. D., & Rees, M. J. 1980, *Nature*, 287, 307
- Blecha, L., & Loeb, A. 2008, *MNRAS*, 390, 1311
- Brown, W. R., Geller, M. J., Kenyon, S. J., & Bromley, B. C. 2009, *ApJ*, 690, L69
- Chen, X., Liu, F. K., & Magorrian, J., 2008, *ApJ*, 676, 54
- Donley, J. L., Brandt, W. N., Eracleous, M., & Boller, T. 2002, *AJ*, 124, 1308
- Dotti, M., Salvaterra, R., Sesana, A., Colpi, M., & Haardt, F. 2006, *MNRAS*, 372, 869
- Esquej, P., Saxton, R. D., Freyberg, M. J., Read, A. M., Altieri, B., Sanchez-Portal, M., & Hasinger, G. 2007, *A&A*, 462, 49
- Haehmelt, M. G. 1994, *MNRAS*, 269, 199
- Hairer, E., Norsett, S. P., & Wanner, G. 1987, *Solving Ordinary Differential Equations I* (Berlin: Springer-Verlag)
- Hills, J. 1975, *ApJ*, 254, 295
- Hughes, S. A. 2002, *MNRAS*, 331, 805
- Innanen, K. A., Zheng, J. Q., Mikkola, S., & Valtonen, M. J. 1997, *AJ*, 11, 1915
- Ivanov, P. B., Polnarev, A. G., & Saha, P. 2005, *MNRAS*, 358, 1361
- Kiseleva, L. G., Eggleton, P. P., & Mikkola, S. 1998, *MNRAS*, 300, 292
- Komossa, S. 2002, *Rev. Mod. Astron.*, 15, 27
- Kozai, Y. 1962, *AJ*, 67, 591
- Levin, Y. 2006, *ApJ*, 653, L1203
- Lippai, Z., Frei, Z., & Haiman, Z. 2008, *ApJ*, 676, L5
- Liu, F. K., 2004, *MNRAS*, 347, 1357
- Liu, F. K. & Chen, X., 2007, *ApJ*, 671, 1272
- Liu, F. K., Wu, X. B., & Cao, S. L., 2003, *MNRAS*, 340, 411
- Madau, P., & Quataert, E. 2004, *ApJ*, 606, L17
- Merritt, D., & Ekers, R. D., 2002, *Sci*, 297, 1310
- Milosavljević, M., & Phinney, E. S. 2005, *ApJ*, 622, L93
- Perets, H. B. 2009, *ApJ*, 690, 795
- Quinlan, G. D. 1996, *New A*, 1, 35
- Rees, M. J. 1988, *Nature*, 333, 523
- Schodel, R., et al. 2007, *A&A*, 469, 125
- Sesana, A., Haardt, F., Madau, P., & Volonteri, M. 2004, *ApJ*, 611, 623
- Sesana, A., Haardt, F., Madau, P., & Volonteri, M. 2005, *ApJ*, 623, 23
- Sesana, A., Haardt, F., & Madau, P. 2006, *ApJ*, 651, 392
- Sesana, A., Haardt, F., & Madau, P. 2007, *ApJ*, 660, 546
- Sesana, A., Haardt, F., & Madau, P. 2008, *ApJ*, 686, 432
- Shields, G. A., & Bonning, E. W. 2008, *ApJ*, 682, 758

Volonteri, M., Haardt, F., & Madau, P. 2003, *ApJ*, 582, 559
Volonteri, M., & Madau, P. 2008, *ApJ*, 687, L57
Wang, J., & Merritt, D., 2004, *ApJ*, 600, 149
Wyithe, J. S. B., & Loeb, A. 2003, *ApJ*, 590, 691

Yu, Q., & Tremaine, S. 2003, *ApJ*, 599, 1129